Theory of acceptor-ground-state description and hot photoluminescence in cubic semiconductors

A. V. Malyshev, I. A. Merkulov, and A. V. Rodina
A. F. Ioffe Physicotechnical Institute, Russian Academy of Sciences, 194021 St. Petersburg, Russia
(Received 3 June 1996)

An approach to the theory of the acceptor ground state in cubic semiconductors is presented. The model has been developed within the framework of the four-band effective Luttinger Hamiltonian and is applicable for both Coulomb and non-Coulomb acceptors. The system of integral equations for the ground-state wave functions has been derived and its solution has been numerically computed. We present the general form of the acceptor-ground-state wave function. The wave functions for a set of acceptor dopants in GaAs are calculated with an accuracy of 2%. The obtained wave functions have been used for qualitative and quantitative analysis of the hot photoluminescence (HPL) spectra and linear polarization in GaAs crystals. Analytical expressions for the line shape and anisotropy of the linear polarization degree have been derived. The dependencies of the HPL characteristics on the excitation energy as well as on the acceptor binding energy have been analyzed. The HPL theory presented allows us to describe the wide spectrum of available experimental data. [S0163-1829(97)07904-6]

I. INTRODUCTION

Investigation of hot photoluminescence (HPL) is important for understanding the behavior of hot charge carriers the energy of which is many times higher than thermal kinetic energy.[1–9] In recent years the HPL lineshape, dependencies of HPL polarization characteristics on excitation energy, and depolarization of HPL in magnetic field have been studied in order to determine the times of energy and momentum relaxation for hot carriers,[3,6–8] the position of energy bands,[8,9] the effect of the higher energy band states on the selection rules of optical transitions,[4,5] and so on.

At low temperatures HPL is mostly determined by the recombination of photoexcited carriers (electrons or holes) with the intrinsic carriers localized at impurity centers. Matrix element of such optical transition is determined by Fourier image of the impurity state wave function at the spatial frequency corresponding to the carrier wave vector **k**. Thus, one has to know the wave function of the localized carriers in the momentum representation for the theoretical description of the available experimental data and the evaluation of hot carriers parameters.

The relatively simple case of a donor center in diamondlike semiconductors is well studied for Coulomb binding potential[10] as well as for a more complicated potential given by a sum of the Coulomb term and a short-range potential.[11] A similar calculation for the localized hole meets essential difficulties resulting from the complexity of the valence band structure and cubic symmetry of the crystal lattice.[10,12–20] That is why up to the present time the HPL characteristics in p-type A_3B_5 semiconductors have been calculated only on the basis of simplified models of the acceptor ground state.[2,4–6,8,17,21]

A theoretical description of the HPL at high excitation energies was performed in Refs. 2,4,5 by using the asymptotic expressions for an acceptor wave function. Such an approximation is valid when the electron wavelength is many times smaller than the Bohr radius of the heavy hole at the acceptor level ($\lambda \ll a_B$). This condition takes place only for very high electron energies corresponding to excitation energies higher than that studied in the known experiments.

At considerably smaller excitation energies the wavelength of a hot electron is of the order of a heavy hole Bohr radius ($\lambda \geqslant a_B$). The acceptor wave functions for corresponding wave vector values were calculated numerically for a Coulomb[18] and a non-Coulomb acceptor[15,17] in spherical approximation. The implementation of the spherical acceptor functions limits the application of the results to the description of experimental data on the linear polarization anisotropy of the HPL. In particular, it does not clarify the question of how the acceptor-ground-state anisotropy influences the HPL polarization characteristics.

Unexpected results were obtained in Refs. 6–8. The authors of these papers apply the simplest hydrogenlike model in the effective mass approximation for the description of the HPL intensity spectra and the determination of the electron intra- and intervalley scattering times in GaAs. It turns out that the simple hydrogenlike wave function describes the experimental data obtained in Refs. 6,8 better than the spherical wave function which has been numerically calculated for GaAs:Zn in Refs. 15,17. The inadequacy of the matrix elements calculated by Dymnikov, Perel, and Polupanov[17] for describing the data from Refs. 6,8 might have resulted from the neglect of a cubic symmetry of the crystal lattice. Besides, these functions were calculated for Zn-acceptor whereas the experiment was carried out for GaAs:Be. However, in the present paper we show that the hydrogenlike model does not provide good agreement with experimental data if the effect of the absorption of the luminescence radiation in the sample is taken into account.

It follows from the brief review of experimental and theoretical papers presented above that for quantitative description of the HPL in diamondlike semiconductors one has to know accurate acceptor wave functions in the wide range of the wave vectors. The warping of the valence band and the deviation of binding potential from the Coulomb form are essential for such a description.

Recently a method of calculation of a Coulomb[19] and a

non-Coulomb[20] acceptor ground state wave function Ψ was reported. Its main advantage is that a simple analytical dependence of the wave function on the direction of wave vector $\mathbf{k}$ with respect to the crystallographic axes has been obtained for all wave vector values. Therefore, the wave functions can be applied for a qualitative description and quantitative analysis of the HPL characteristics in a considerably wide range of excitation energies. Analytical expressions for the HPL line shape, linear polarization degree, and its anisotropy in cubic semiconductors were derived in Ref. 21. These expressions contain numerical coefficients which depend on the acceptor-ground-state wave function. The Coulomb acceptor functions, numerically calculated in Ref. 19, were used to study the dependencies of the HPL characteristics on the excitation energy $\hbar\omega_{\rm exc}$ in GaAs crystals.[21]

In this paper we present a complete theory of both the Coulomb and the non-Coulomb acceptor ground state in diamondlike semiconductors with large spin-orbit coupling. The theory is applied for the studying of the hot photoluminescence characteristics.

The paper is organized as follows. In Sec. II the model of the acceptor ground state is described. The model takes into account the complex structure of the valence band of cubic semiconductors as well as a deviation of an impurity potential from Coulomb form. A general form of the acceptor-ground-state wave function Ψ is found on the basis of the model. The system of integral equations for the wave function is derived in momentum representation. In Sec. III the method of numerical solution of the system is described. The results of numerical calculations of the acceptor-ground-state wave functions and acceptor eigenenergies (for Coulomb acceptors) for different semiconductors and acceptors are presented and discussed. In Sec. IV the general analytical expressions for matrix elements of optical transition in cubic semiconductors are derived. In Sec. V the HPL characteristics in GaAs crystals are calculated and compared with available experimental and theoretical data. The brief summary of the results obtained is given in Sec. VI.

II. THEORY OF ACCEPTOR GROUND STATE IN CUBIC SEMICONDUCTORS

In this section we consider the model of the acceptor ground state in diamondlike semiconductor with a large value of spin-orbit splitting. The binding potential is presented as the sum of a Coulomb potential and a short-range one. The cubic symmetry of the crystal lattice is taken into account.

The Schrödinger equation for a hole bound to an acceptor impurity can be written in a momentum representation as follows:

$$\hat{H}_L(\mathbf{k})\Psi(\mathbf{k})-\frac{e^2}{2\pi^2\varepsilon}\int\frac{d^3\mathbf{q}}{(\mathbf{k}-\mathbf{q})^2}\Psi(\mathbf{q}) - \int d^3\mathbf{q}V(\mathbf{k}-\mathbf{q})\Psi(\mathbf{q})=E_a\Psi(\mathbf{k}), \tag{1}$$

where $\hat{H}_L(\mathbf{k})$ is the four-band Luttinger Hamiltonian,[22] E_a is a binding energy, $\Psi(\mathbf{k})$ and $V(\mathbf{k})$ are Fourier images of the wave function $\Psi(\mathbf{r})$ and short-range potential $V(\mathbf{r})$:

$$\Psi(\mathbf{k})=\int d^3\mathbf{r}\exp[-i\mathbf{kr}]\Psi(\mathbf{r}),$$

$$V(\mathbf{k})=\int d^3\mathbf{r}\exp[-i\mathbf{kr}]V(\mathbf{r}). \tag{2}$$

$\Psi(\mathbf{k})$ is a four-component column written in the basis of Bloch functions of the valence band top u_μ ($\mu=\pm 3/2, \pm 1/2$). The second term on the left side of Eq. (1) describes the Coulomb attraction of a hole to an acceptor core. The third one describes the action of non-Coulomb part of the potential.

The ground state of an acceptor in cubic semiconductors is fourfold degenerate and has the symmetry of the top of the valence band.[10] The wave function for the four sublevels can be found in the form

$$\Psi_M(\mathbf{k})=\hat{P}(\mathbf{k})u_M, \quad (M=\pm 3/2,\pm 1/2), \tag{3}$$

where the operator $\hat{P}(\mathbf{k})$ is invariant under transformations of the cubic symmetry of the crystal. We will seek the operator $\hat{P}$ in the following general form (the error of this approximation will be estimated later):

$$\hat{P}(\mathbf{k})=[f_h(\mathbf{k})\hat{\Lambda}_h(\mathbf{k})+f_l(\mathbf{k})\hat{\Lambda}_l(\mathbf{k})], \tag{4}$$

$$\hat{\Lambda}^{l,h}=\mp\frac{\hat{H}_L(\mathbf{k})-E_{h,l}(\mathbf{k})}{E_h(\mathbf{k})-E_l(\mathbf{k})}, \tag{5}$$

where $f_{h,l}(\mathbf{k})$ are some cubic symmetric functions depending only on wave vector $\mathbf{k}$. The operators $\hat{\Lambda}^{l,h}$ are the projection operators on the light- and heavy-hole subband states with dispersion laws $E_{l,h}$:

$$E_{l,h}=\frac{\hbar^2k^2}{2m_{l,h}(\mathbf{k})}, \quad m_{l,h}(\mathbf{k})=\frac{m_0}{\gamma_1\pm 2\gamma_2\alpha(\mathbf{k})}, \tag{6}$$

$$\alpha(\mathbf{k})=\frac{m_0}{2\hbar^2k^2\gamma_2}[E_l(\mathbf{k})-E_h(\mathbf{k})] = \sqrt{1+3v\frac{k_x^2k_y^2+k_y^2k_z^2+k_z^2k_x^2}{k^4}}, \tag{7}$$

where γ_1, γ_2, and γ_3 are Luttinger parameters[22] and $v=(\gamma_3^2-\gamma_2^2)/\gamma_2^2$ is the warping parameter of the valence band.

The cubic symmetric function $\alpha(\mathbf{k})$ plays an important role in the further analysis of the dependencies of the functions $f_{h,l}$ on the wave vector direction and for the analytical description of hot photoluminescence. This function depends only on the $\mathbf{k}$ orientation with respect to crystallographic axes and takes the value between the unit for $\mathbf{k}$ parallel to [001]-direction and $\sqrt{1+v}=\gamma_3/\gamma_2$ for $\mathbf{k}$ parallel to the [111] direction.

The square modules of the functions $f_h^2(\mathbf{k})$ and $f_l^2(\mathbf{k})$ present the distribution of the bound hole state over the states of free holes in the valence band. For the wave function Ψ in the form (3, 4) the normalization condition gives [the crystal volume is $(2\pi)^3$]:

$$\frac{1}{2}\int d^3\mathbf{k}[f_h^2(\mathbf{k})+f_l^2(\mathbf{k})]=1. \tag{8}$$

Let us substitute the function Ψ in the form (3, 4) into the Schrödinger equation (1). The explicit form of a non-Coulomb part of the acceptor binding potential is unknown. Assuming the short-range potential $V(\mathbf{r})$ to have the symmetry of the crystal cell and the potential radius r_0 to be considerably less than the acceptor-ground-state radius r_a (so that the value $kr_0 \ll 1$), one can rewrite the non-Coulomb integral term in the following way:

$$\begin{aligned}\int d^3\mathbf{q}V(\mathbf{k}-\mathbf{q})P(\mathbf{q}) &= \int d^3\mathbf{r}\exp[-i\mathbf{kr}]V(\mathbf{r}) \\ &\times \int \boldsymbol{d}^3\mathbf{q}\exp[i\mathbf{qr}]P(\mathbf{q}) \\ &\approx \int d^3\mathbf{q}\int d^3\mathbf{r}\exp[i\mathbf{qr}]V(\mathbf{r})P(\mathbf{q}) \\ &= A\hat{I}, \end{aligned} \tag{9}$$

where $\hat{I}$ is a unit matrix and A is some constant.

It is readily seen that both operator $\hat{H}_L(\mathbf{k})P(\mathbf{k})$ and non-Coulomb integral term (9) can be exactly expanded in terms of $\hat{\Lambda}^{h,l}(\mathbf{k})$. Thus the error of approximation (4) arises only due to the fact that the Coulomb integral operator $\int \boldsymbol{d}^3\mathbf{q}/(\mathbf{k}-\mathbf{q})^2 P(\mathbf{q})$ has no precise expansion in terms of $\hat{\Lambda}^{h,l}(\mathbf{k})$. The error of such an expansion was shown to be about 2%.[19] [It is noteworthy that in the framework of spherical approximation the solution (4) is the exact one.] Operating on Eq. (1) by the projection operators (5) one can obtain the system of equations for the functions $f_h(\mathbf{k})$ and $f_l(\mathbf{k})$ with an accuracy of 2% (the detailed description of this procedure can be found in Ref. 20):

$$\begin{aligned}[E_h(\mathbf{k})-E_a]f_h(\mathbf{k}) &= \frac{e^2}{4\pi^2\varepsilon}\int \frac{d^3\mathbf{q}}{(\mathbf{k}-\mathbf{q})^2}f_h(\mathbf{q})\left[1+\frac{L(\mathbf{k},\mathbf{q})}{\alpha(\mathbf{k})\alpha(\mathbf{q})}\right] \\ &+ \frac{e^2}{4\pi^2\varepsilon}\int \frac{d^3\mathbf{q}}{(\mathbf{k}-\mathbf{q})^2}f_l(\mathbf{q}) \\ &\times\left[1-\frac{L(\mathbf{k},\mathbf{q})}{\alpha(\mathbf{k})\alpha(\mathbf{q})}\right] \\ &+ A[E_l(\mathbf{k})-E_a]f_l(\mathbf{k})] \\ &= \frac{e^2}{4\pi^2\varepsilon}\int \frac{d^3\mathbf{q}}{(\mathbf{k}-\mathbf{q})^2}f_h(\mathbf{q})\left[1-\frac{L(\mathbf{k},\mathbf{q})}{\alpha(\mathbf{k})\alpha(\mathbf{q})}\right] \\ &+ \frac{e^2}{4\pi^2\varepsilon}\int \frac{d^3\mathbf{q}}{(\mathbf{k}-\mathbf{q})^2}f_l(\mathbf{q}) \\ &\times\left[1+\frac{L(\mathbf{k},\mathbf{q})}{\alpha(\mathbf{k})\alpha(\mathbf{q})}\right]+A. \end{aligned} \tag{10}$$

where $L(\mathbf{k},\mathbf{q}) = P_2(\cos(\theta)) + 3v(k_xk_yq_xq_y + k_yk_zq_yq_z + k_zk_xq_zq_x)/(k^2q^2)$, θ is an angle between $\mathbf{k}$ and $\mathbf{q}$, and P_2 is the Legendre polynomial.

The system (10) describes the ground state of a hole bound at an acceptor center in a fourfold degenerate valence band of the Γ_8 type. The warping of the isoenergy surfaces as well as the deviation of the acceptor binding potential from Coulomb form are taken into account.

The shallow acceptor state can be described in the framework of the Coulomb model by homogeneous system resulting from (10) with constant $A\equiv 0$. Its solution gives the eigenenergy E_a^{Coulomb} and eigenfunction of the Coulomb acceptor. The deep acceptor states with $E_a \gg E_a^{\text{Coulomb}}$ can be described by the implementation of a short-range potential model.[23] Then the Coulomb integral terms in system (10) are neglected. In this case the wave functions of the acceptor state with a given binding energy can be obtained in an analytical form:

$$f_{l,h}(\mathbf{k})=\frac{A}{E_{l,h}(\mathbf{k})-E_a}, \tag{11}$$

where the constant $A=A(E_a)$ comes from the normalization condition (8).

The complete solution of the system (10) gives the acceptor-ground-state wave functions $f_{h,l}(\mathbf{k})$ in all range of the directions and values of the wave vector. It can be easily seen from (10) that the contribution from heavy- and light-hole states are equal at small k values: $f_l(0)=f_h(0)$. The asymptotic expressions for the functions $f_{l,h}(\mathbf{k})$ follow from (10): $f_{l,h}(\mathbf{k})\propto m_{l,h}(\mathbf{k})/k^2$. They are different from those known for Coulomb acceptor:[19,2] $f_{l,h}(\mathbf{k})\propto m_{l,h}(\mathbf{k})/k^4$.

In the following we use dimensionless units and functions:

$$\varepsilon=-\frac{E_a}{E_B},\quad \mathbf{p}=\mathbf{k}a_B,\quad \tilde{f}_{h,l}=f_{h,l}a_B^{-3/2},\quad \tilde{A}=\frac{A}{E_Ba_B^{3/2}}$$

$$E_B=\frac{e^4m_h^0}{2\varepsilon\hbar^2},\quad a_B=\frac{\varepsilon\hbar^2}{e^2m_h^0},\quad m_h^0=\frac{m_0}{\gamma_1-2\gamma},$$

$$\gamma=\frac{2\gamma_2+3\gamma_3}{5}, \tag{12}$$

$$g_1(\mathbf{p})=\tilde{f}_h(\mathbf{p})+\tilde{f}_l(\mathbf{p}),\quad g_2(\mathbf{p})=\frac{\tilde{f}_h(\mathbf{p})-\tilde{f}_l(\mathbf{p})}{\alpha(\mathbf{p})}. \tag{13}$$

Here m_h^0 is heavy-hole (HH) mass in the spherical approximation, E_B is HH Bohr energy, and a_B is HH Bohr radius. For the new functions and units the system takes the form

$$\begin{aligned}[\varepsilon_1(p)+\varepsilon]g_1(\mathbf{p})-\alpha^2(\mathbf{p})\varepsilon_2(p)g_2(\mathbf{p}) &= \frac{1}{\pi^2}\int \frac{d^3\mathbf{q}}{(\mathbf{p}-\mathbf{q})^2}g_1(\mathbf{q})+2\tilde{A}, \\ -\alpha^2(\mathbf{p})\varepsilon_2(p)g_1(\mathbf{p})+\alpha^2(\mathbf{p})[\varepsilon_1(p)+\varepsilon]g_2(\mathbf{p}) &= \frac{1}{\pi^2}\int \frac{d^3\mathbf{q}}{(\mathbf{p}-\mathbf{q})^2}g_2(\mathbf{q})L(\mathbf{p},\mathbf{q}), \end{aligned} \tag{14}$$

where

$$\varepsilon_1(p)=\frac{1+\beta}{2\beta}p^2,\quad \varepsilon_2(p)=\frac{1-\beta}{2\beta}\frac{5}{2+3\sqrt{1+v}}p^2,$$

$$\beta=\frac{\gamma_1-2\gamma}{\gamma_1+2\gamma}. \tag{15}$$

As it has been mentioned above the non-Coulomb part of the potential and then the constant A is unknown. We assume that the real acceptor binding energy E_a is known from the experiment and use it as the given parameter in order to obtain the acceptor-ground-state wave functions. Let us seek the real acceptor functions in the form $g_{1,2}=\widetilde{A}\widetilde{g}_{1,2}$, where the functions $\widetilde{g}_{1,2}$ satisfy the system (14) with constant $\widetilde{A}=1$ and can be computed numerically. The constant $\widetilde{A}$ can be calculated by using the normalization condition:

$$\widetilde{A}=\widetilde{A}(\varepsilon)=\frac{1}{4}\left(\int d^3\mathbf{p}[\widetilde{g}_1^2(\mathbf{p})+\alpha^2(\mathbf{p})\widetilde{g}_2^2(\mathbf{p})]\right)^{-1/2}. \tag{16}$$

So, $\widetilde{A}$ plays the role of a normalization constant, although it contains information about the short-range potential and differs for different dopants.

III. CALCULATION METHODS AND RESULTS

In this section we present the calculation methods which have been used for solving Eq. (14) and discuss the obtained results. Since the functions $f_{h,l}$ and then $g_{1,2}$ are cubic scalars, they can be expanded into cubic harmonics.[19] This method allows us to derive the dependence of the wave function on wave vector direction analytically, but it converges slowly at large values of $\mathbf{p}$. We will combine the method of expansion into cubic harmonics together with a fast convergent iteration method in a order to get an accurate solution in a wide range of the wave vector values.

Presenting the system (14) in the operator form

$$\hat{G}(\varepsilon)\mathbf{g}=\hat{K}\mathbf{g}+\widetilde{A}\mathbf{b},\quad \mathbf{g}=\begin{pmatrix}g_1(\mathbf{p})\\ g_2(\mathbf{p})\end{pmatrix},\quad \mathbf{b}=\begin{pmatrix}2\\0\end{pmatrix}, \tag{17}$$

where $\hat{G}$ is the operator of the left part of (14), $\hat{K}$ is the integral operator from (14), we derive the iteration expression for the functions $\widetilde{\mathbf{g}}=\mathbf{g}/\widetilde{A}$:

$$\widetilde{\mathbf{g}}^{(n+1)}=\hat{G}^{-1}\hat{K}\widetilde{\mathbf{g}}^{(n)}+\hat{G}^{-1}\mathbf{b}, \tag{18}$$

where n is the number of iteration. Let us seek the zeroth-order approximation $\widetilde{\mathbf{g}}^{(0)}$ in the form of the expansion into cubic harmonics up to the harmonic of the fourth order:

$$\widetilde{\mathbf{g}}^{(0)}=\begin{pmatrix}\widetilde{g}_1^0(p)T_0(\Omega_p)+\widetilde{g}_1^4(p)T_4(\Omega_p)\\ \widetilde{g}_2^0(p)T_0(\Omega_p)+\widetilde{g}_2^4(p)T_4(\Omega_p)\end{pmatrix}, \tag{19}$$

where Ω_p is solid angle, $T_0(\Omega_p)$, $T_4(\Omega_p)$ are cubic harmonics:[24]

$$T_0(\Omega_p)=Y_{00}(\Omega_p)=\frac{1}{2\sqrt{\pi}},$$

$$T_4(\Omega_p)=\frac{1}{2}\sqrt{\frac{5}{6}}[Y_{4-4}(\Omega_p)+Y_{44}(\Omega_p)]+\frac{1}{2}\sqrt{\frac{7}{3}}Y_{40}(\Omega_p), \tag{20}$$

where $Y_{lm}(\Omega_p)$ are spherical harmonics. The functions $\widetilde{g}_{1,2}^{0,4}(p)$ depend only on wave vector module and are the solutions of the following system:

$$\begin{aligned}
&[\varepsilon_1(p)+\varepsilon]\widetilde{g}_1^0(p)-b_1\varepsilon_2(p)\widetilde{g}_2^0(p)+b_3\varepsilon_2(p)\widetilde{g}_2^4(p)\\
&\quad=\frac{2}{\pi}\int_0^\infty q^2dqM_1(p,q)\widetilde{g}_1^0(q)+4\sqrt{\pi}b_3\varepsilon_2(p)\widetilde{g}_2^0(p)\\
&\qquad+[\varepsilon_1(p)+\varepsilon]\widetilde{g}_1^4(p)-b_2\varepsilon_2(p)\widetilde{g}_2^4(p)\\
&\quad=\frac{2}{\pi}\int_0^\infty q^2dqM_3(p,q)\widetilde{g}_1^4(q)-b_1\varepsilon_2(p)\widetilde{g}_1^0(p)+b_1[\varepsilon_1(p)+\varepsilon]\widetilde{g}_2^0(p)+b_3\varepsilon_2(p)\widetilde{g}_1^4(p)-b_3[\varepsilon_1(p)+\varepsilon]\widetilde{g}_2^4(p)\\
&\quad=\frac{2}{\pi}\left[b_1\int_0^\infty q^2dqM_2(p,q)\widetilde{g}_2^0(q)-b_3\int_0^\infty q^2dqM_2(p,q)\widetilde{g}_2^4(q)\right]b_3\varepsilon_2(p)\widetilde{g}_1^0(p)\\
&\qquad-b_3[\varepsilon_1(p)+\varepsilon]\widetilde{g}_2^0(p)-b_2\varepsilon_2(p)\widetilde{g}_1^4(p)+b_2[\varepsilon_1(p)+\varepsilon]\widetilde{g}_2^4(p)\\
&\quad=\frac{2}{\pi}\left[-b_3\int_0^\infty q^2dqM_2(p,q)\widetilde{g}_2^0(q)+\int_0^\infty q^2dqM_4(p,q)\widetilde{g}_2^4(q)\right],
\end{aligned} \tag{21}$$

where

$$b_1=(1+0.6v),\quad b_2=\left(1+\frac{321}{715}v\right),\quad b_3=\frac{1.2v}{\sqrt{21}}, \tag{22}$$

$$M_{1,2,3}(p,q)=\frac{1}{pq}Q_{0,2,4}\left(\frac{p^2+q^2}{2pq}\right),$$

$$\begin{aligned}
M_4(p,q)=&\frac{1}{pq}Q_4\left(\frac{p^2+q^2}{2pq}\right)P_2\left(\frac{p^2+q^2}{2pq}\right)\\
&+\frac{v}{pq}\left[\frac{4}{35}Q_2\left(\frac{p^2+q^2}{2pq}\right)+\frac{60}{847}Q_4\left(\frac{p^2+q^2}{2pq}\right)\right.\\
&\left.+\frac{415}{1573}Q_6\left(\frac{p^2+q^2}{2pq}\right)\right],
\end{aligned} \tag{23}$$

TABLE I. Valence band parameters and acceptor binding energies in diamondlike semiconductors.

Semicond.	æ (Ref. 13)	γ_1 (Ref. 13)	γ_2 (Ref. 13)	γ_3 (Ref. 13)	E_a^{Coulomb} (meV)	E_a (meV) (Ref. 25)	$\tilde{A}$
Ge	15.36	13.35	4.25	5.69	10.36	10.8 (B)	5.74×10^{-3}
InSb	17.9	35.08	15.64	16.91	9.26	9.25 (Ge)	7.92×10^{-5}
InP	12.4	6.28	2.08	2.76	37.81	41.3 (C)	1.23×10^{-2}
GaP	10.75	4.20	0.98	1.66	50.63	54.3 (C)	8.65×10^{-3}
GaAs	12.56	7.65	2.41	3.28	27.35	27.0 (C)	1.72×10^{-3}
						28.0 (Be)	3.17×10^{-3}
						29.0 (Mg)	8.05×10^{-3}
						31.0 (Zn)	1.77×10^{-2}
						40.0 (Ge)	5.84×10^{-2}

where P_2 is Legendre polynomial, and Q_l are Legendre functions of the second type. This system is self-consistent and can be solved numerically. Calculating the constant $\tilde{A}$ with the help of (16) one can obtain the normalized zeroth-order approximation of the wave function.

Our analysis shows that the error of this approximation grows with p. It is less than 2% in the region $p \leqslant p_c \sim \sqrt{\varepsilon}$, and is about 10% for $p \gg p_c$. On the other hand, the integral values such as the normalization constant $\tilde{A}$ or eigenenergies of Coulomb acceptor can be calculated with an accuracy of about 2% in the zeroth-order approximation. As a matter of fact the region of the maximum error makes a small contribution to the corresponding integrals as the absolute value of the wave function is very small.

To get a more accurate solution for the wave function let us make the first iteration according to Eq. (18). The system (21) can be conveniently written in the operator form:

$$\hat{G}_0\tilde{\mathbf{g}}^{(0)} = \hat{K}_0\tilde{\mathbf{g}}^{(0)} + \mathbf{b}. \tag{24}$$

The error connected with the expansion of the term $\hat{K}\tilde{g}^{(0)}$ into cubic harmonics T_0 and T_4 appeared to be less than 2%. This makes it possible to simplify the expression for the first-order approximation. If one puts $\hat{K}\tilde{g}^{(0)} = \hat{K}_0\tilde{g}^{(0)}$ and substitutes $\hat{K}_0\tilde{g}^{(0)}$ into (18) a very simple expression for the first-order approximation can be obtained:

$$\tilde{\mathbf{g}}^{(1)} = \hat{G}^{-1}\hat{G}_0\tilde{\mathbf{g}}^{(0)}. \tag{25}$$

The accuracy of this approximation is about 2% for all directions and values of **p**. There is no need to continue the iterations because the error connected with the influence of the split-off band usually exceeds several percent.

Thus, we obtained the solution of system (10) for the acceptor-ground-state wave function with an accuracy of 2%. The dependence of the wave functions $f_{h,l}$ on the wave vector direction is derived analytically and can be expressed in terms of $T_0(\mathbf{k})$, $T_4(\mathbf{k})$, and $\alpha(\mathbf{k})$. It is noteworthy that the function $\alpha^2(\mathbf{k})$ can be expressed in terms of cubic harmonics T_0 and T_4 exactly:

$$\alpha^2(\mathbf{k}) = 2\sqrt{\pi}b_1T_0(\Omega_k) - 2b_3T_4(\Omega_k). \tag{26}$$

It allows us to conclude that the cubic anisotropy of the functions $f_{h,l}(\mathbf{k})$ is defined by the anisotropy of the valence band also with an accuracy of a 2%:

$$f_{h,l}(\mathbf{k}) = f_{h,l}(k,\alpha(\mathbf{k})) = f_{h,l}\left(k, \frac{m_0}{2\hbar^2k^2\gamma_2}[E_l(\mathbf{k}) - E_h(\mathbf{k})]\right). \tag{27}$$

This fact appears to be very helpful in deriving the expressions for matrix elements of optical transitions.

Table I shows Coulomb acceptors-ground-state eigenenergies E_a^{Coulomb} numerically calculated for different semiconductors. The sets of Luttinger parameters used and experimental values of the acceptor binding energies E_a are also shown. The energies calculated with cubic symmetry of the crystal lattice taken into account differ from those obtained in the framework of spherical approximation[13,12] by 6–8 %. The results agree well with calculations of Ref. 16. One can see from Table I that in the cases of Ge, InSb, and GaAs the model of Coulomb acceptor provides good agreement for shallow acceptors (such as Ge:B, InSb:Ge, GaAs:C, GaAs:Be). In the cases of InP and GaP the discrepancy may be due to both the large central cell corrections and the imperfection of the present model that assumes a large spin-orbit splitting of the valence band. In the case of GaAs the difference for deeper acceptors (Zn, Ge) is due to the considerable central cell corrections. The last column of Table I presents the values of the dimensionless constant $\tilde{A}$, calculated from (16) for the acceptors presented. This parameter contains information on the short-range potential.

The acceptor-ground-state distribution functions $f_{h,l}^2(k)$ for the Coulomb acceptor (upper set) and the non-Coulomb Zn acceptor (lower set) in GaAs are displayed in Fig. 1. Pairs of solid lines in each set correspond to $f_h^2(k)$ (upper curve in the pair) and $f_l^2(k)$ (lower curve in the pair) for the [111] direction while dashed lines correspond to [001] direction. The function f_h^2 is very anisotropic while f_l^2 is nearly spherical. The ratio of the functions f_h^2 for directions [111] and [001] at $k \approx a_B^{-1}$ is about 2.4. The same ratio of the functions f_l^2 is close to 1.2. It can be seen from Fig. 1 that even for the shallow Zn acceptor the wave functions are different from Coulomb ones at small values of wave vector k. The asymptotic behavior of Coulomb and non-Coulomb distribution functions at $k \gg a_B^{-1}$ is also different. Figure 2 presents the functions $f_{h,l}^2(k)$ (with **k** parallel to [011] direction) for a number of acceptors in GaAs. These functions differ strongly at small values of k and are very close in the region $k \approx a_B^{-1}$ that is the most important for the description of the HPL process.

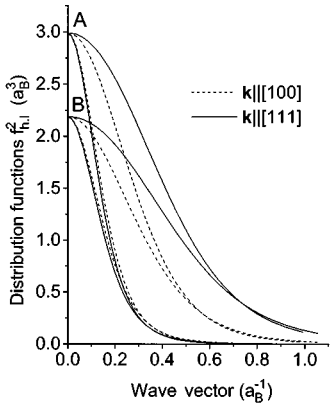

FIG. 1. Acceptor-ground-state distribution functions $f^2_{h,l}(\mathbf{k})$ in the Coulomb model (set A) and in the non-Coulomb model (set B) for GaAs:Zn. The upper curve of each pair corresponds to $f^2_h(\mathbf{k})$; the lower curve corresponds to $f^2_l(\mathbf{k})$. Hereafter, the values of $\mathbf{k}$ are given in a_B^{-1} and the values of $f^2_{h,l}$ are in a_B^3, where $a_B = 11.8$ Å.

IV. THEORY OF THE HPL IN CUBIC SEMICONDUCTORS

The implementation of the acceptor-ground-state wave functions obtained in the previous section allows us to calculate the components of the fourth-rank tensor $\hat{A}$ which gives the most general relationship between polarizations of the exciting light and the recombination luminescence:

$$\langle E_i^l E_j^{l*}\rangle = A_{ijkn}\langle E_k^{\rm ex} E_n^{\rm ex*}\rangle, \tag{28}$$

where $E_i^{\rm ex}$ and E_i^l are components of the electric field vectors of laser and luminescence, respectively. The angle brackets mean a time average. One has to know the tensor $\hat{A}$ components for a theoretical description of the line shape (the dependence of the total detected intensity I on HPL energy $\hbar\omega_{\rm lum}$) and HPL polarization characteristics. In cubic crystal only four components of the tensor $\hat{A}$ are linearly independent. They are $A_{iiii}=A_{11}$, $A_{iijj}=A_{12}$, $A_{ijij}=A_{44}$, and $A_{ijji}=A_{47}$, where $i,j=x,y,z$ and $i\neq j$. All other components are equal to zero.

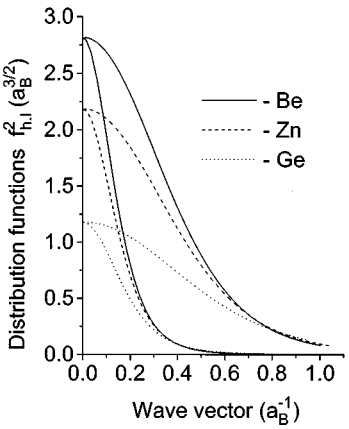

FIG. 2. Acceptor-ground-state distribution functions $f^2_{h,l}(\mathbf{k})$ for the [011] direction in GaAs.

If totally polarized exciting light and detected radiation propagate along the [001] direction the degree of linear polarization ρ_l has the form:[4]

$$\rho(\varphi)=\frac{I_\parallel - I_\perp}{I_\parallel + I_\perp}=\frac{d+c}{2a}+\frac{d-c}{2a}\cos(4\varphi), \tag{29}$$

where $I_\parallel$ and $I_\perp$ are the luminescence intensities polarized parallel and perpendicular to the polarization vector $\mathbf{e}_{\rm exc}$ of the exciting light, and φ is the angle between $\mathbf{e}_{\rm exc}$ and [100]. The coefficients a, c, and d can be derived from components of the tensor $\hat{A}$: $a=A_{11}+A_{12}$, $c=A_{44}+A_{47}$, and $d=A_{11}-A_{12}$. The value $\zeta=\rho_{45}/\rho_0=\rho(\pi/4)/\rho(0)=d/c$ characterizes the anisotropy of the HPL linear polarization.

The process of hot photoluminescence consists of two steps. At the first step an electron transits from valence band to conduction band, and at the second the electron recombines optically with a hole bound to an acceptor center. If the electron is not scattered by phonons, the final wave vector is equal to the initial one. In this case one can derive the components of the tensor $\hat{A}$ in the form

$$A_{kn}^{h,l}=\int A_{kn}^{h,l}(\mathbf{k})\,\delta[\hbar\omega_{\rm lum}-E_g+E_a-E_c(k)] \times\delta[\hbar\omega_{\rm exc}-E_g-E_c(k)-E_{h,l}(\mathbf{k})]d^3\mathbf{k}, \tag{30}$$

where the tensor $\hat{A}(\mathbf{k})$ characterizes the recombination of electron at wave vector $\mathbf{k}$, E_g is the band gap, E_a is the acceptor binding energy, $E_c(k)=\hbar^2k^2/2m_e$ is the electron energy in the conduction band with effective mass m_e, $E_{h,l}(\mathbf{k})$ is the energy of a heavy or light hole in the valence band (6). Indexes h and l correspond to excitation from the heavy- and light-hole subbands, respectively. Integration is carried out over all directions of the wave vector $\mathbf{k}$.

Integral (30) with integrand $A_{kn}(\hat{G}\mathbf{k})$, where $\hat{G}$ is the arbitrary transformation of the point group of the crystal lattice is equal to the integral with integrand $A_{kn}(\mathbf{k})$ due to the cubic invariance of the tensor $\hat{A}$ in cubic semiconductors. It can be easily seen that values $A_{kn}(\mathbf{k})=\Sigma A_{kn}(\hat{G}\mathbf{k})/N$, where the summation is carried out over all N cubic transformations, are cubic scalars in the cubic semiconductors. Thus, the components of the tensor $\hat{A}$ can be derived by evaluating the integrals of the form (30) with the cubic invariant integrand $A_{kn}(\mathbf{k})$, which is more convenient.

Using the general form of the acceptor-ground-state wave functions (3), (4) found in Sec. II we can derive components of the tensor $\hat{A}(\mathbf{k})$. Here we present the results of such a derivation for the values $\overline{a}(\mathbf{k})=A_{11}(\mathbf{k})+A_{12}(\mathbf{k})$, $\overline{c}(\mathbf{k})=A_{44}(\mathbf{k})+A_{47}(\mathbf{k})$, and $d(\mathbf{k})=A_{11}(\mathbf{k})-A_{12}(\mathbf{k})$:

$$\overline{a}_{h,l}(\mathbf{k})=\frac{8}{9}[f_h^2(\mathbf{k})+f_l^2(\mathbf{k})] \pm\frac{v+1-\alpha^2(\mathbf{k})}{9v\,\alpha^2(\mathbf{k})}[f_h^2(\mathbf{k})-f_l^2(\mathbf{k})], \tag{31}$$

$$\overline{c}_{h,l}(\mathbf{k}) = \pm\frac{2(v+1)[\alpha^2(\mathbf{k})-1]}{9v\alpha^2(\mathbf{k})}[f_h^2(\mathbf{k})-f_l^2(\mathbf{k})],$$

$$\overline{d}_{h,l}(\mathbf{k}) = \pm\frac{v+1-\alpha^2(\mathbf{k})}{9v\alpha^2(\mathbf{k})}[f_h^2(\mathbf{k})-f_l^2(\mathbf{k})].$$

By substituting these functions into (30) we find the quantities a, c, and d. In expressions (31) all cubic scalar coefficients are expressed in terms of the function $\alpha(\mathbf{k})$. The plus and minus signs correspond to the excitation from the heavy-hole and light-hole subband, respectively. Hereinafter we concentrate on describing the first nonphonon peak in the HPL spectra that corresponds to the excitation from the heavy-hole subband. The high-frequency edge $\omega_{\rm lum}^{\rm max}$ and the low-frequency edge $\omega_{\rm lum}^{\rm min}$ of this peak are associated with the recombination of electrons with $\mathbf{k}$ parallel to the [111] and [100] directions, respectively. The width of HPL line $\Delta\hbar\omega_{\rm lum}$ depends on the excitation energy.[4]

It is clear that for a fixed excitation energy $\hbar\omega_{\rm exc}$ the nonzero contributions to the integral (30) at the luminescence energy $\hbar\omega_{\rm lum}$ come only from those directions and magnitudes of the wave vector $\mathbf{k}$ which lie at the intersection of the excitation surface $\Omega_{\rm exc}$ defined by the equation $\hbar\omega_{\rm exc}-E_g-E_c(k)-E_{h,l}(\mathbf{k})=0$ and the luminescence sphere of the radius $k_0=[2m_e(\hbar\omega_{\rm lum}-E_g+E_a)/\hbar^2]^{1/2}$. Thus, the modulus of the wave vector and the function $\alpha(\mathbf{k})$ take the definite values at the integration contour.[26] It has been shown in Sec. III that in our model the distribution functions $f_{h,l}(\mathbf{k})$ depend only on the modulus of the wave vector k and the function $\alpha(\mathbf{k})$ with an accuracy of 2%. In this case integrands (31) remain constant along the integration contour and can be factored out from the integral. So, an integral of type (30) can be simplified:

$$X=\overline{X}(k_0,\alpha_{\rm exc})W(\hbar\omega_{\rm lum}), \quad X=a,c,d, \tag{32}$$

where $\alpha_{\rm exc}=\gamma_1/2\gamma_2-[(\hbar\omega_{\rm exc}-E_g)/(\hbar\omega_{\rm lum}-E_g+E_a)-1]m_0/2\gamma_2 m_e$, and function W is the density of states integrated over the contour:

$$W(\hbar\omega_{\rm lum})=\frac{4\pi\alpha_{\rm exc}}{\gamma_2 v\sqrt{(\hbar\omega_{\rm lum}-E_g+E_a)/(2m_e)}}T(t_{\rm exc}),$$

$$t_{\rm exc}=\frac{\alpha_{\rm exc}^2-1}{v}, \tag{33}$$

$$T(t)=\frac{1}{\pi}\int_{G(t)}\frac{dx}{\sqrt{(t-3x^2+3x^4)(3/4-t+3/2x^2-9/4x^4)}}. \tag{34}$$

Here the function $G(t)$ is the intersection of the line segment $[0;1]$ with the region in which the integrand is defined. The value of the parameter $t_{\rm exc}$ varies from zero at the low-frequency edge ($\omega_{\rm lum}=\omega_{\rm lum}^{\rm min}$) to unity at the high-frequency edge ($\omega_{\rm lum}=\omega_{\rm lum}^{\rm max}$). The function T is independent of excitation energy as well as of semiconductor parameters. Its main features are as follows (see solid curve at Fig. 3): the function diverges logarithmically at $t_{\rm exc}\to 3/4$ and remains finite at all other values of the parameter $t_{\rm exc}$. The values of $T(t_{\rm exc})$ at the edges of the $[0;1]$ segment are $T(0)=1$ and $T(1)=2$. It is very important to note here that although the function diverges at $t_{\rm exc}\to 3/4$ the integral of the function over $[0;1]$ is finite.

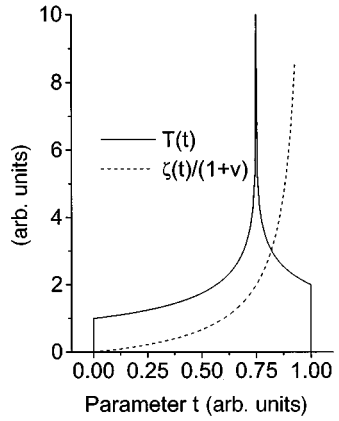

FIG. 3. The function $T(t)$ which determines the main features of the HPL line (solid curve) and the distribution of the linear polarization anisotropy over the HPL line $\zeta(t)$ divided by $(1+v)$ (dashed curve).

The HPL intensity spectrum $I=I_\parallel+I_\perp\propto a$ and the difference spectra $I_{[100]}^-=I_\parallel-I_\perp\propto d$ ($\mathbf{e}_{\rm exc}\|[100]$) and $I_{[110]}^-=I_\parallel-I_\perp\propto c$ ($\mathbf{e}_{\rm exc}\|[110]$) are determined by expressions (31–33). The HPL line shape depends on excitation energy, acceptor binding energy, and semiconductor parameters, but its main features are determined by the function $T(t_{\rm exc})$: the low- and high-frequency edges are characterized by steps of different height while the point $t_{\rm exc}=3/4$ is characterized by the divergence of the spectra. Maxima of the spectra correspond, in particular, to the recombination of electrons with $\mathbf{k}$ parallel to [011] direction. It is noteworthy that no such spectral features are observed in reality due to spectra broadening caused by different mechanisms such as the finite hot electron lifetime or acceptor-ground-state energy level broadening. These mechanisms lead to a smoothing of the spectra singularities and to a shift of the spectra maximums.

Expressions for the HPL polarization follow from (31,32):

$$\rho_0(t_{\rm exc})=\frac{3(1-t_{\rm exc})\beta_0(k_0,\alpha_{\rm exc})}{8(vt_{\rm exc}+1)+(1-t_{\rm exc})\beta_0(k_0,\alpha_{\rm exc})},$$

$$\rho_{45}(t_{\rm exc})=\frac{2(v+1)t_{\rm exc}\beta_0(k_0,\alpha_{\rm exc})}{8(vt_{\rm exc}+1)+(1-t_{\rm exc})\beta_0(k_0,\alpha_{\rm exc})}, \tag{35}$$

$$\beta_0(k_0,\alpha_{\rm exc})=\beta_0(\mathbf{k}_0)=\frac{f_h^2(\mathbf{k}_0)-f_l^2(\mathbf{k}_0)}{f_h^2(\mathbf{k_0})+f_l^2(\mathbf{k_0})},$$

$$\alpha_{\rm exc}=\sqrt{1+vt_{\rm exc}}, \tag{36}$$

here the function $\beta_0(\mathbf{k}_0)$ characterizes the difference between the relative contributions of the heavy- and light-hole states to the acceptor-ground-state wave function. One can see from (35) that linear polarization degree ρ_0 vanishes at the high-frequency edge ($t_{\rm exc}=1$), while ρ_{45} vanishes at the low-frequency edge ($t_{\rm exc}=0$). The dependencies of the degree of linear polarization on the excitation energy and acceptor binding energy are determined by the function β_0.

TABLE II. Experimental data and calculated values of the linear polarization degrees ρ_0 (a) and ρ_{45} (b) and anisotropy of linear polarization ζ (c) at the maximum of the HPL line. Brackets with index a denote values averaged over the broadened acceptor line ($\Delta E_a = 13$ meV).

(a)

$\hbar\omega_{ex}$ (eV)	ρ_0^{exp} (Refs. 4 and 5)	ρ_0	$\langle\rho_0\rangle_a$	$\langle\rho_0\rangle_a$ (Ref. 4)
1.65	0.07	0.051	0.069	0.08
1.92	0.04	0.053	0.052	0.03

(b)

$\hbar\omega_{ex}$ (eV)	ρ_{45}^{exp} (Refs. 4 and 5)	ρ_{45}	$\langle\rho_{45}\rangle_a$	$\langle\rho_{45}\rangle_a$ (Ref. 4)
1.65	0.18	0.189	0.182	0.19
1.92	0.26	0.198	0.199	0.26

(c)

$\hbar\omega_{ex}$ (eV)	ζ^{exp} (Refs. 4 and 5)	ζ	$\langle\zeta\rangle_a$	$\langle\zeta\rangle_a$ (Ref. 4)
1.65	2.57	3.75	2.64	2.36
1.92	6.50	3.75	3.85	8.67

We point out here that for the wave vectors involved to the HPL process (e.g., $k \geqslant 0.6a_B^{-1}$ for GaAs) the contribution from the light-hole states to the shallow acceptor wave function is small. In the case $[f_l(\mathbf{k})/f_h(\mathbf{k})]^2 \ll 1$ the function

$$\beta_0(\mathbf{k}) \approx 1 - 2\left[\frac{f_l(\mathbf{k})}{f_h(\mathbf{k})}\right]^2$$

is nearly isotropic. Consequently the degree of HPL linear polarization weakly depends on the cubic anisotropy of acceptor distribution functions $f_{l,h}^2(\mathbf{k})$ and can be calculated to within a 5% error by using the spherical distribution functions. This fact was demonstrated for high excitation energies in Ref. 4 by numerical calculations carried out with asymptotic anisotropic and isotropic distribution functions.

On the other hand, the value of the function $\beta_0(\mathbf{k})$ for shallow acceptors deviates from its asymptotic value

$$\beta_\infty(\mathbf{k}) = \frac{m_h^2(\mathbf{k}) - m_l^2(\mathbf{k})}{m_h^2(\mathbf{k}) + m_l^2(\mathbf{k})}$$

by less than 5% when the contribution from light-hole states is small. It is noteworthy that the asymptotic function β_∞ has the same form in any model of the acceptor impurity potential and does not depend on the module of wave vector k. For this reason any type of distribution function is applicable for evaluating the linear polarization degree to within a 5% error at high excitation energies. Using the asymptotic function $\beta_\infty(\mathbf{k})$ in expressions (35) one can calculate the asymptotic value of the HPL linear polarization degree analytically.

The degree of linear polarization anisotropy of the HPL $\zeta = \rho_{45}/\rho_0 \equiv I^-_{[011]}/I^-_{[001]}$ varies over the luminescence line from zero at the low-frequency edge of the HPL peak to infinity at the high-frequency edge and depends only on the valence band warping parameter v:

$$\zeta(t_{exc}) = \frac{2(1+v)t_{exc}}{3(1-t_{exc})}, \quad 1+v \equiv \frac{\gamma_3^2}{\gamma_2^2}. \tag{37}$$

Dashed curve at Fig. 3 presents the function $\zeta(t)/(1+v)$ which does not depend on the semiconductor parameters. We emphasize that ζ depends neither on excitation energy nor on the acceptor distribution functions. The anisotropy of the linear polarization appears only due to the valence band warping and its value contains no information about the anisotropy of the acceptor-ground-state distribution functions. The account of broadening mechanisms leads only to a weak dependence of ζ on the excitation energy and the acceptor binding energy.

The essential features of the HPL spectrum, described above, are universal for diamond-like semiconductors with a large value of spin-orbit splitting. At high excitation energies the effect of the spin-orbit split-off band cannot be neglected and leads to qualitative changes in the spectra features as well as to a considerable increase of the linear polarization anisotropy.[4,5]

V. THE HPL CHARACTERISTICS FOR GAAS

The HPL linear polarization and its anisotropy were experimentally studied in Refs. 4,5 for two excitation energies $\hbar\omega_{exc} = 1.65$ and 1.92 eV.[4,5] The experiment was carried out for GaAs crystal doped with Zn acceptors. The theoretical polarization characteristics of the HPL in GaAs:Zn are presented in Table II together with experimental data. The degrees of linear polarization ρ_0 and ρ_{45} and anisotropy parameter ζ are calculated at the HPL line maximum. To obtain a more accurate comparison with the experimental data the corresponding values averaged over the broadening acceptor level have been calculated (see the values in angle brackets). The acceptor linewidth (the full width at half maximum of the acceptor line) is taken as $\Delta E_a = 13$ meV according to Ref. 5. The distribution of acceptors over the energy levels are supposed to be Gaussian. The other possible mechanism of the spectrum broadening connected with fluctuations of the band gap width has also been considered, but was found to produce no noticeable corrections to the polarization characteristics. One can see from Table II that the present model

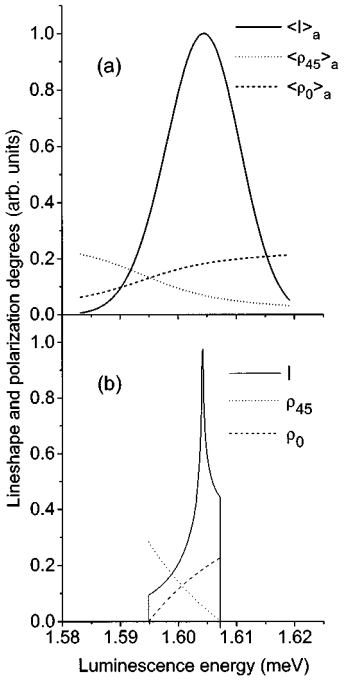

FIG. 4. HPL characteristics calculated without (a) and with (b) account for the acceptor level broadening $\Delta E_a = 13$ meV for GaAs:Zn at $\hbar\omega_{\rm exc} = 1.65$ eV.

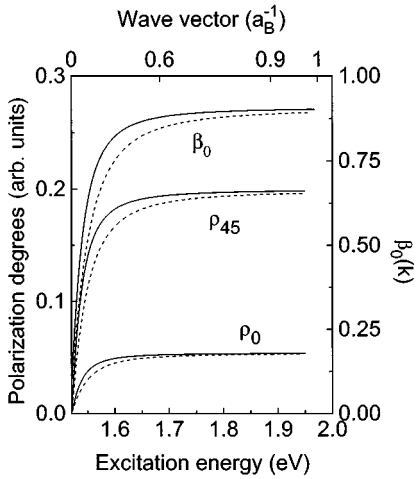

FIG. 5. Dependence of function $\beta(\mathbf{k}_0)$ for the [011] direction and degrees of linear polarization ρ_{45} and ρ_0 at the HPL spectra maximum on excitation energy for GaAs:Zn (solid curves) and GaAs:Ge (dashed curves).

provides excellent agreement with the experimental data at excitation energy $\hbar\omega_{\rm exc} = 1.65$ eV. Table II presents also the HPL characteristics numerically calculated in Ref. 4 by using the asymptotic expressions for the acceptor wave functions. The model developed in Ref. 4 takes into account the effect of the spin-orbit split-off band. It allows us to describe the increase in the degree of linear polarization anisotropy at high excitation energy $\hbar\omega_{\rm exc} = 1.92$ eV.

The HPL line shape and distribution of the linear polarization degree over the luminescence line, calculated within the model presented for GaAs:Zn at $\hbar\omega_{\rm exc} = 1.65$ eV, are shown at Fig. 4(a). Figure 4(b) presents the line shape and degree of the linear polarization averaged over a broadened acceptor level.

The dependencies of the linear polarization degree ρ_0 and ρ_{45} at the HPL spectra maximum on the excitation energy for GaAs:Zn and GaAs:Ge are shown in Fig. 5. It illustrates also the functions $\beta_0(\mathbf{k}_0)$ for $\mathbf{k}_0$ parallel to the [110] direction. One can see that the qualitative behavior of the linear polarization degree is determined by the behavior of the function β_0. For wave vector $k \approx 0.6 a_B^{-1}$ (it corresponds to $\hbar\omega_{\rm exc} \approx 1.65$ eV), the contribution of the light-hole subband states to the shallow acceptor wave function is small. Thus the deviation of β_0 as well as the degree of linear polarization from its asymptotic value is less than 5%. As the excitation energy decreases ($\hbar\omega_{\rm exc} \leqslant 1.65$ eV) the contribution of light-hole states to the acceptor wave function increases. That leads to a decrease of the linear polarization degree. At the same time the degree of anisotropy $\zeta = \rho_{45}/\rho_0$ remains constant independently of an admixture of the light-hole states. At the line maximum it is equal to $\zeta = 2(\upsilon + 1) = 2\gamma_3^2/\gamma_2^2 = 3.75$ (see the parameters of GaAs in Table I). The degree of anisotropy defined by an average over the broadened acceptor line intensities

$$\langle\zeta\rangle_a = \langle\rho_{45}\rangle_a / \langle\rho_0\rangle_a = \langle I^-_{[110]}\rangle_a / \langle I^-_{[100]}\rangle_a$$

depends weakly on the excitation energy and the acceptor binding energy. This dependence is more pronounced at low excitation energies, when the acceptor linewidth ΔE_a is of the same order of magnitude as the HPL linewidth $\Delta E_{\rm lum}$.

The anisotropy of the HPL linear polarization degree and its dependence on excitation energy was also experimentally studied in Ref. 8. The difference spectra $I^-_{[100]}$ and $I^-_{[110]}$ were presented for excitation energy $\hbar\omega_{\rm exc} = 1.5978$ eV for GaAs:C. The maximum of the $I^-_{[100]}$ difference spectrum was noticed to be at a lower energy than the maximum of the $I^-_{[110]}$ spectrum. The intensity ratio of difference spectra was detected to be about 4 (which gives the degree of linear polarization anisotropy). This ratio increases up to about 6 as the laser energy increases to 1.7510 eV. In the framework of the present theory the line shapes of the difference spectra are determined by the function T. As a result the spectra have their maxima at the same point determined by the value $t_{\rm exc} = 3/4$. The degree of linear polarization anisotropy varies along the line and is equal to 3.75 at the point of the spectra maximum which is independent of excitation energy. The shift of the difference spectra maxima may appear due to some broadening mechanism. Figure 6 illustrates, for example, the difference spectra calculated for GaAs:C at $\hbar\omega_{\rm exc} = 1.5978$ eV with acceptor level broadening $\Delta E_a = 5$ meV. Such broadening leads to a maxima shift of 2.5 meV corresponding to the data of Ref. 8. As was mentioned above, the increase of the anisotropy degree is connected with the effect of the spin-orbit split-off band and cannot be described in our model.

The dependence of the integrated intensity of the first HPL peak on the excitation energy was measured and analyzed in Refs. 6,8 in order to estimate the intervalley electron scattering time in GaAs. The experiment was carried out for several GaAs samples doped with different shallow acceptors (C, Be, Mg, Zn). The intensities were compared pairwise

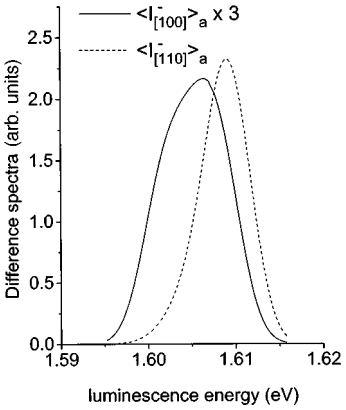

FIG. 6. Difference spectra calculated taking into account the acceptor level broadening $\Delta E_a = 5$ meV for GaAs:C at $\hbar\omega_{\rm exc} = 1.5978$ eV.

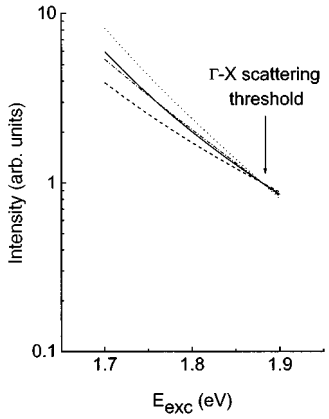

FIG. 7. The dependence of the HPL intensity (integrated area) on the excitation energy for GaAs:Be calculated without (solid and dashed curves) and with (dotted and dot-dashed curves) account for the reabsorption effect in the hydrogenlike (EMA) model (solid and dotted curves) and the present model (dashed and dot-dashed curves). All curves are scaled to pass through the same data at $\hbar\omega_{\rm exc} = 1.88$ eV.

as the laser energy was changed over the region 1.6–2.0 eV. The comparison showed no difference from the experiment to within the $\pm 5\%$ error.[8] Our calculations of the integrated intensity show the difference for shallow acceptors in GaAs less than 10% in good agreement with the experimental data. Such small difference between the curves is due to the fact that the wave functions of different acceptors are very close to each other in the region of wave vectors corresponding to these excitation energies (see Fig. 2 at $k \sim a_B^{-1}$). A straightforward calculation shows that for deeper acceptor GaAs:Ge the difference increases.

According to Refs. 6,8 the experimental dependence measured for GaAs:Be can be approximated by the function

$$I \propto |M(k)|^2 \tau n,$$

where n is the probability that an electron is actually born in the conduction band by the absorption of a photon with energy $\hbar\omega_{\rm exc}$, τ is an electron lifetime which is considered to be independent of excitation energy below the Γ-L scattering threshold (i.e., for $\hbar\omega_{\rm exc} \leqslant 1.88$ eV). The acceptor wave function is defined in the hydrogenlike model by

$$|M(k)| \propto \left(1 + \frac{\hbar^2 k^2}{2E_a m_a}\right)^{-2}, \tag{38}$$

where m_a is a hole mass in the effective mass approximation (EMA) [$m_a = 0.31 m_0$, $E_a = 27$ meV in GaAs (Ref. 6)]. On the other hand, the alternative expression for $|M(k)|$, based on spherical acceptor wave functions for GaAs:Zn, numerically calculated by Dymnikov, Perel', and Polupanov,[17] was reported to be in bad agreement with the experimental data.[6,8]

It should be noted that the good agreement of the hydrogenlike EMA model (38) of the HPL intensity dependence on excitation energy is just an accidental coincidence. As a matter of fact, this dependence is affected by a lot of supplementary factors (such as the absorption of the luminescence radiation in the sample, the Coulomb interaction between electrons and holes,[27] the effect of the higher energy band states on the selection rules of optical transitions,[4,5] the changing of the absorption depth with excitation energy, and others) that were not taken into account in Refs. 6,8. It can be shown by straightforward calculations (its description is beyond the scope of this paper) that the effect of reabsorption, for instance, plays an important role. This effect reduces the number of detected photons and is essential at high excitation energies when the free path of hot electrons becomes the same order as the absorption depth. Figure 7 presents the dependencies of the integrated HPL intensity on the excitation energy, calculated within the hydrogenlike EMA model (solid and dotted curves) and our model (dashed and dot-dashed curves) without (solid and dashed curves) and with (dotted and dot-dashed curves) the effect of reabsorption (the influence of the Coulomb interaction between a hot electron and a hole on the absorption depth is also taken into account). As was indicated in Ref. 6, the solid curve describes well the experimental data below the intervalley scattering threshold corresponding to 1.88 eV. At the same time the exact calculation for GaAs:Be (dashed curve) (as well as the result of calculations performed with spherical acceptor distribution functions for GaAs:Zn) differs significantly. As is evident from Fig. 7, this situation changes when the effect of the reabsorption is taken into account: the difference between EMA model (dotted curve) and experiment data (indicated by a solid curve) increases while the exact calculation (dot-dashed curve) provides a good description at excitation energies 1.7–1.88 eV.

Thus, the proper description of the HPL experimental data demands taking into account a complex structure of the valence band when calculating the acceptor ground state wave functions. The admixture of the light hole states to the acceptor wave function is more essential for the region of low excitation energies, while at high excitation energies the heavy-hole states contribution dominates. As a result one can use the asymptotic distribution functions for evaluating the degree of linear polarization at high excitation energies but not for the description of the HPL spectra. The cubic anisotropy of the acceptor distribution functions is essential for detailed description of the HPL spectra. However, it does not affect the anisotropy of the linear polarization. In the range of wave vectors involved in the HPL process the model of a

Coulomb acceptor as well as a short-range potential center can provide a good agreement with the experimental data. Thus, the present model is a more general one than the previous models[2,17,4,19] and allows us to describe properly a wide spectrum of the available experimental data.[4–6,8]

VI. CONCLUSION

Let us summarize now the main results of the present paper.

(1) We obtained analytically and solved numerically a system of integral equations for the ground-state wave functions of a cubic non-Coulomb acceptor in diamond-like semiconductors. A general form of the acceptor-ground state-wave function has been found and the wave functions for a set of acceptor dopants in GaAs have been calculated with an accuracy of 2%.

(2) The dependence of the acceptor wave functions on the direction of the wave vector $\mathbf{k}$ with respect to crystallographic axes has been derived analytically for arbitrary values of k and an acceptor binding energy. It has been shown that the acceptor distribution functions $f^2_{h,l}(\mathbf{k})$ are cubic scalars and depend with an accuracy of 2% on the value of wave vector modulus k and cubic scalar function $\alpha(\mathbf{k})$ which determines the cubic anisotropy of the valence band dispersion $E_{h,l}(\mathbf{k})$.

(3) The analytical theory of the line shape and linear polarization anisotropy of the HPL has been developed. The principal futures of the HPL spectrum are found to be universal for cubic semiconductors with large spin-orbit splitting: (A) A maximum of the first nonphonon peak, resulting from excitation from the heavy-hole subband, corresponds, in particular, to the recombination of the electron with wave vector $\mathbf{k}$ parallel to $[011]$ direction. As far as the HPL polarization characteristics are determined by the function $\alpha(\mathbf{k})$, they can be obtained at the spectra maximum by evaluating the matrix elements of optical transitions for all equivalent $\langle 011 \rangle$ directions only. (B) The dependence of the linear polarization degree on the excitation energy and acceptor binding energy is determined by the function β_0 which characterizes the difference between the relative contribution of the heavy- and light-hole subband states to the acceptor wave function. At high excitation energies, when the contribution of the light-hole states is negligible, the values of linear polarization degree are independent of the excitation energy and the acceptor binding energy. For lower energies admixture of the light-hole states leads to a decrease of the linear polarization degree. (C) The anisotropy of linear polarization degree is determined solely by valence band warping and contains no information about the anisotropy of the acceptor distribution functions. In the framework of the present model its value ζ does not depend on excitation energy. However, such a dependence occurs due to an additional mechanism of spectra broadening and the effect of the spin-orbit split-off band.

(4) Quantitative characteristics of the HPL in p-GaAs crystals calculated in the framework of the present model are shown to be in good agreement with the available experimental data (Refs. 4–6,8).

ACKNOWLEDGMENTS

We would like to thank B.P. Zacharchenya, V.I. Perel', D.N. Mirlin, and I.I. Reshina for helpful discussions. The research described in this publication was made possible in part by Grant No. JF2100 from International Science Foundation and Russian Government and by Grant No. 950204055 from Russian Foundation of Fundamental Investigation.

[1] D. N. Mirlin and I. I. Reshina, Zh. Eksp. Teor. Fiz. **73**, 859 (1977) [Sov. Phys. JETP **46**, 451 (1977)].
[2] V. D. Dymnikov, D. N. Mirlin, V. I. Perel', and I. I. Reshina, Fiz. Tverd. Tela (Leningrad) **20**, 2165 (1978) [Sov. Phys. Solid State **20**, 1250 (1978)].
[3] B. P. Zakharchenya, D. N. Mirlin, V. I. Perel', and I. I. Reshina, Usp. Fiz. Nauk. **136**, 459 (1982) [Sov. Phys. Usp. **25**, 143 (1982)].
[4] M. A. Alekseev *et al.*, Fiz. Tverd. Tela (Leningrad) **27**, 2650 (1985) [Sov. Phys. Solid State **27**, 1589 (1985)].
[5] M. A. Alekseev *et al.*, Phys. Lett. **A 127**, 373 (1988).
[6] R. G. Ulbrich, J. A. Kash, and J. C. Tsang, Phys. Rev. Lett. **62**, 949 (1989).
[7] J. A. Kash, Phys. Rev. B **40**, 3455 (1989).
[8] J. A. Kash, Phys. Rev. B **47**, 1221 (1993).
[9] M. Zachau, J. A. Kash, and W. T. Masselink, Phys. Rev. B **44**, 4048 (1991).
[10] G. L. Bir and G. E. Pikus, *Symmetry and Strain-Induced Effects in Semiconductors* (Halsted, Jerusalem, 1974).
[11] L. D. Landau and E. M. Lifshitz, *Quantum Mechanics* (Pergamon Press, New York, 1989).
[12] B. L. Gel'mont and M. I. Dyakonov, Fiz. Tekh. Poluprovodn. **5**, 2191 (1971) [Sov. Phys. Semicond. **5**, 1905 (1972)].
[13] A. Balderesci and N. O. Lipari, Phys. Rev. B **8**, 2697 (1973).
[14] A. Balderesci and N. J. Lipari, Phys. Rev. B **9**, 1525 (1974).
[15] Sh. M. Kogan and A. F. Polupanov, Fiz. Tekh. Poluprovodn. **13**, 2338 (1979) [Sov. Phys. Semicond. **13**, 1368 (1979)].
[16] A. F. Polupanov and R. Taskinboev, Fiz. Tekh. Poluprovodn. **22**, 112 (1988) [Sov. Phys. Semicond. **22**, 68 (1988)].
[17] V. D. Dymnikov, V. I. Perel', and A. F. Polupanov, Fiz. Tekh. Poluprovodn. **16**, 235 (1982) [Sov. Phys. Semicond. **16**, 148 (1982)].
[18] B. L. Gel'mont and A. V. Rodina, Fiz. Tekh. Poluprovodn. **25**, 2189 (1991) [Sov. Phys. Semicond. **25**, 1319 (1991)].
[19] I. A. Merkulov and A. V. Rodina, Fiz. Tekh. Poluprovodn. **28**, 321 (1994) [Sov. Phys. Semicond. **28**, 195 (1994)].
[20] A. V. Malyshev, I. A. Merkulov, and A. V. Rodina, Fiz. Tekh. Poluprovodn. **30**, 159 (1996) [Sov. Phys. Semicond. **30**, 91 (1996)].
[21] I. A. Merkulov and A. V. Rodina, Fiz. Tekh. Poluprovodn. **28**, 1268 (1994) [Sov. Phys. Semicond. **28**, 720 (1994)].
[22] J. M. Luttinger, Phys. Rev. **102**, 1030 (1956).
[23] V. I. Perel' and I. N. Yassievich, Zh. Eksp. Teor. Fiz. **82**, 237 (1982) [Sov. Phys. JETP **55**, 143 (1982)].

[24] D. T. Sviridov and Yu. F. Smirnov, *The Theory of the Optical Spectra of Transition Metals* (Nauka, Moscow, 1977).

[25] *Physics of Group IV Elements and III-V Compunds*, edited by K.-H. Hellwege and O. Madelung, Landolt-Börnstein, New Series, Group III, Vol. 17, Pt. a (Springer-Verlag, Berlin, 1982).

[26] We would like to note here that several directions of the wave vector may correspond to the same value of the function $\alpha(\mathbf{k})$. In other words $\alpha(\mathbf{k})$ does not unambiguously define the direction of the wave vector.

[27] I. A. Merkulov, Fiz. Tekh. Poluprovodn. **25**, 351 (1991) [Sov. Phys. Semicond. **25**, 214 (1991)].